DISCUSSION ON MECHANICAL BEHAVIOUR OF CRANIAL IMPLANT THROUGH FE SIMULATION BASED ON CT IMAGES

Abstract

Construction of patient's specific cranial implant with a porous structure improves the implant design, surgical planning, implant-tissue interaction and surgeon's accuracy. In the last few decades, even though many researches have underwent in developing bio implant materials for cranioplasty, surgeons are still facing difficulties in developing optimal design for safe and more accurate reconstruction of cranial implant. In this study, CT SCAN containing voxel data based DICOM images of the patient skull is converted into triangle data based STL file. The temporal damaged portion of the skull is reconstructed into a 3D patient specific cranial implant using available commercial software. The mechanical performance of reconstructed cranial implant with different bio - implant materials (Poly Ether Ether Ketone (PEEK), Poly Methyl Metha Acrylate (PMMA) and Titanium alloy (Ti6Al4V)) and external deformity by two fixture conditions (8 and 10 fixation points) has been carried by finite element study. The results reveals that, Ti6Al4V shows less deformation and PEEK exhibit lesser equivalent stress under 15 mm Hg of intracranial pressure when compared to other selected bio - materials.

Keywords: Cranial implant, Biomaterials, Image Segmentation, Finite Element Analysis.

Authors

Karthik Narayanan A
Department of Rubber and Plastics Technology
MIT Campus
Anna University
Chennai, Tamilnadu, India.

Mugendiran V
Department of Production Technology
MIT Campus
Anna University
Chennai, Tamilnadu, India.
mugendiran.v@mitindia.edu

I. INTRODUCTION

Cranioplasty is reconstructive surgical process by which defective part on the skull is repaired by specific cranial implant [1-3]. In the seventeenth century, the first true and successful bone graft, which was performed with bone from a dead dog cranium [1]. Although allograft bone transplantation is the best way of cranioplasty but it has some complications, availability of donor, infections and layer complex defect [1-2, 5]. Last few years many of researchers have been working on developing optimal materials with osteo integration and implant model creation [3].

3D modeling of the human anatomy is made possible by advancements in medical image processing technologies, such as CT or MRI. Based on the patient's CT or MRI scan information, a customized cranial implant is created and made [5–6]. DICOM files are composed of a variety of tissues, including skin and bone, and are created by combining a sequence of X-ray images taken at different angles from a CT scan. Transferring into a 3D representation of a particular part is necessary [7-8]. In a DICOM file, picture segmentation aids in the isolation of objects from other images [7, 9–11]. By choosing the proper threshold range, one of the simple methods for creating a binary picture from a grayscale image that has all the necessary information regarding the shape and location of the implant is image segmentation by thresholding. [7, 9-10].

The stereo lithographic type (STL) CAD model, which has a meshed structure with varying face sizes, is saved as a result of the slicer program. It has been discovered that implants with pores are more effective than those without. The implant's pores aid in biomineralization for improved fitting, faster healing, and interfacial adhesion with bone [12–13]. Pore ingrowth should be between 500 and 1500 µm in size for optimal fluid transplantation and cell adherence [13-17]. Although the implant's pores offer numerous benefits, their ability to endure intracranial pressure is limited. The results of the mathematical study of implants show biological scenarios and are consistent with the model's actual functionality. FEA has been used more frequently in the medical field recently to analyze the human musculoskeletal system and to reconstruct biomechanics, evolutionary anthropology, and functional morphology [9, 13, 17–19]. In order to replicate the ideal cranial implant, it is important to investigate the structural alterations and failure behavior of the device under varied load circumstances, fixation points, and intracranial pressure. [2,9,13-15,20].

For cranioplasty, autogenous bone transplantation is the best option, however because of its complications, biomaterial implants are used instead. Common materials used to fabricate patient-specific cranial implants include titanium alloy (Ti6Al4V), polyether ether ketone (PEEK), hydroxyapatite (HA), and polymethyl (PMMA) [1,3]. PMMA is an easily accessible, reasonably priced, biocompatible material that may be 3D printed or molded. When it comes to molds, PMMA is pressed into them and let to cure. With a few small changes, it can be applied to the skull defect after cooling. PMMA has poorer mechanical qualities than cortical bone due to its low elastic modulus and air bubble secretion, which increases infection rates. Ti6Al4V exhibits a higher elastic modulus in comparison to PMMA and PEEK [21]. Owing to his increased stress-shielding action, the implant becomes looser and eventually fails because bone tissue around it absorbs. PEEK is a superior polymer with good mechanical, biological, and chemical properties when compared to other materials [22].

As a result, it can lessen the possibility of osteolysis and bone resorption brought on by the implant's stress shielding action [23]. Its 93.7% success rate in cranioplasty is enhanced by its hardness, fatigue resistance, creep resistance, nontoxic qualities, and sterilizing capabilities. [1, 14, 24-26]. In contrast to conventional techniques, Additive Manufacturing (AM) has become widely used in the production of patient-specific cranial implants through the use of computer-aided design and reverse engineering techniques. [27].

According to the research, the design of the cranial implant heavily depends on the fixation and material characteristics like Young's modulus. We examine three distinct biomaterials under various load and fixation scenarios. The goal of this work is to use finite element simulation to recreate a patient-specific 3D CAD model of the cranium from DICOM pictures by integrating the design and analysis of a personalized cranial implant utilizing CAD tools and reverse engineering techniques..

II. MATERIALS AND METHODOLOGY

1. **Materials:** Bio-implant materials, such as Poly Ether Ether Ketone (PEEK), Poly Methyl Metha Acrylate (PMMA), and Titanium alloy (Ti6Al4V), are taken into consideration in this study. Tables 1 and 2 summarize their mechanical and physical properties. It is assumed that the material has isotropic, homogenous, and linear elastic characteristics.

Table 1: Material Properties of PMMA, PEEK and TI6Al4V

Properties	PEEK	PMMA	Ti6Al4V
Density (gm/cc)	1.31	1.18	4.429
Thermal Conductivity (W/mK)	0.252	0.167 – 0.25	6.7

Table 2: Mechanical Properties of PMMA, PEEK and TI6Al4V

Properties	PEEK	PMMA	Ti6Al4V
Yield Strength (MPa)	100MPa	72 MPa	800 MPa
Young’s Modulus (MPa)	4000MPa	300 MPa	110000MPa
Poisson’s ratio	0.4	0.38	0.3
Flexural strength GPa	4.14	2.9	0.123

2. **Methodology:** Using CT scanning, the patient's cranial defect is scanned to create the CAD model of the implant. The suggested methodology used in this investigation is depicted in Figure 1. The first step is data acquisition, during which the DICOM file format of the CT scan data of the patient with the cranial defect is obtained. This file contains metadata, which is used to reconstruct the CT model, such as slice thickness, spacing between slices, depth, dimensions, etc..

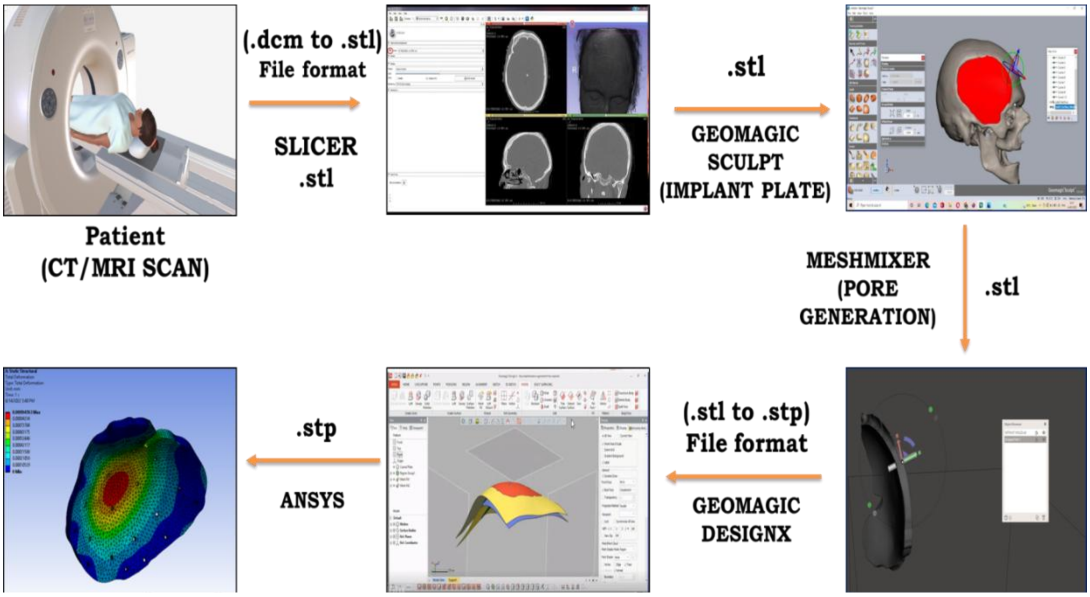

Figure 1: Reconstruction procedure form DICOM images to 3D CAD model

The slicer software's image segmentation and geometric reconstruction techniques aid in the surface representation of a defective skull. A portion of the skull is extracted and stored in Stereo Lithographic (STL) file format by choosing an appropriate threshold range (1000–1500HU). It is simple to derive the patient's unique cranial implant dimensions and contour from this geometric model. The skull portion created from a DICOM file in Slicer program is seen in Figure 2.

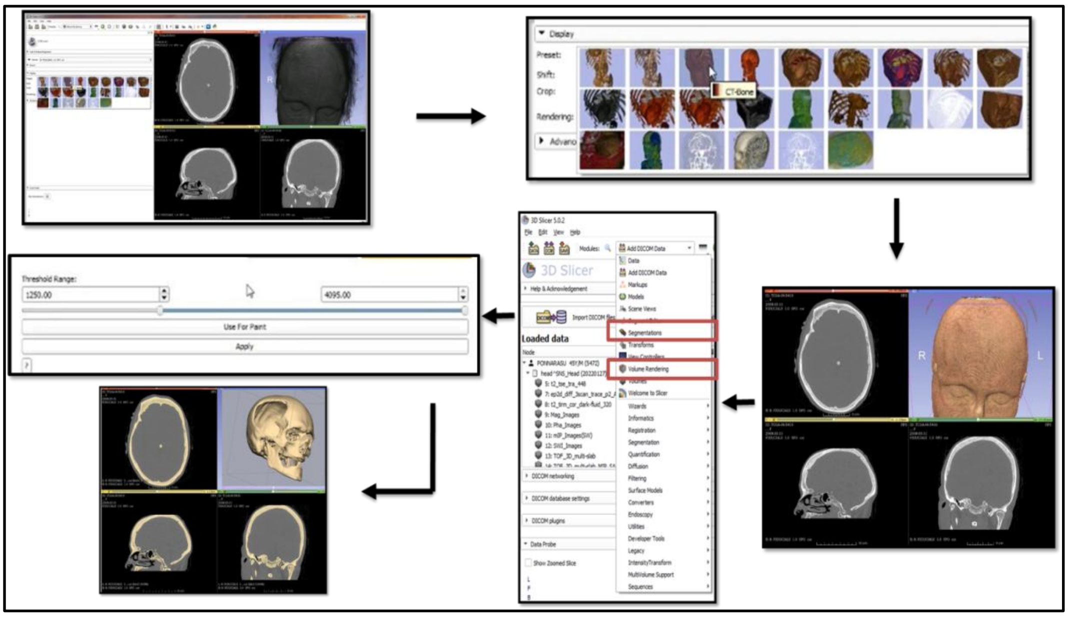

Figure 2: Conversion of skull part using slicer software

After the geometry of the defect is known, the implant that will be implanted is created using the clay modeling approach with the aid of the Geomagic Sculpt software.

The defect is surrounded by a curve line, and a datum plane is introduced at a distance of about 5 mm from the defect that is perpendicular to the z-axis. This datum plane is used to project the 3Curve, which is then extruded as solid clay. A SubD surface covering the flaw is built from this. In accordance with design considerations, the surface is extruded for 4 mm, producing an STL file formatted three-dimensional patient-specific cranial implant model. The created implant's dimensions are slightly changed for a better fit, and it is re-fixed with the missing skull section for correctness. A laser smoothing instrument is used to smooth the implant. The defective skull portion of the GeoMagic Sculpt software is depicted in Figure 3.

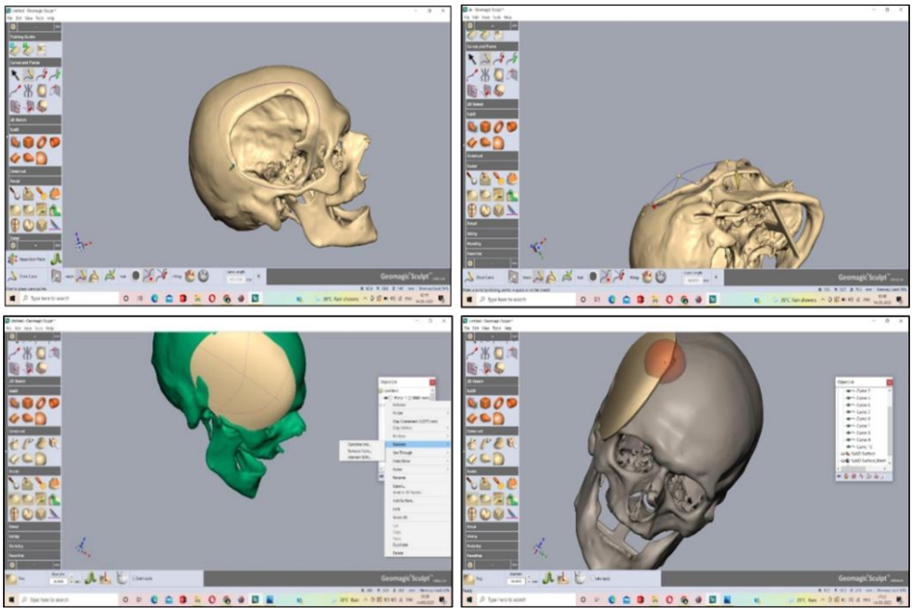

Figure 3: Defective portion of skull part

Blood vessel and mineral circulation occur during the process of skin bio-mineralization that occurs in between the inner dermis of the scalp and skull. Taking this into consideration, the implant is designed with 2 mm diameter pores spaced 20 mm apart to allow for optimal mineral exchange and bone regrowth. The 3D model of a cranial implant created using Autodesk Meshmixer program is displayed in Figure 4.

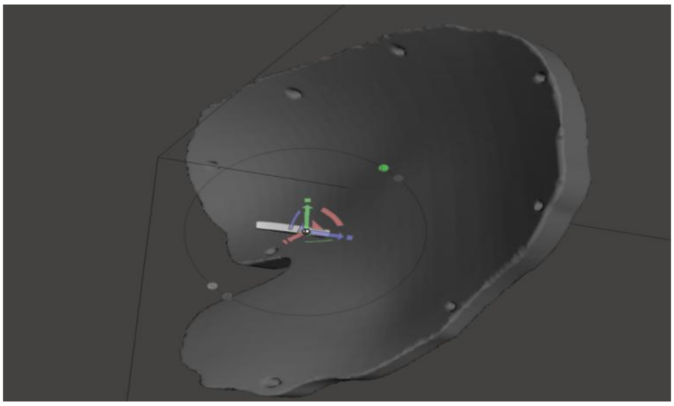

Figure 4: Pore generation on Cranial Implant

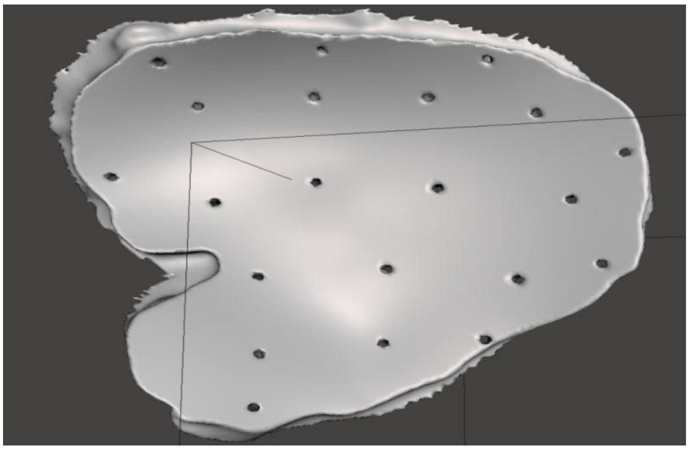

Figure 5: Generated Cranial Implant with pores

The 3D model of a particular cranial implant generated using the outlined is displayed in Figure 5. The model is composed of triangular facets with varying mesh sizes distributed throughout the design. To get around this, the GeoMagic Design X program converts STL files into STEP files. Meshfit and surface primitive are used to create a region on the model's top and bottom layers. On the impressions formed over the top and bottom layers, respectively, a line is drawn. The extrusion command is used to make the edges of the sketch created on the two regions solidify. The cranial implant phase file has now been received for examination. The Geomagic Design X software's 3D model of a cranial implant is shown in Figure 6.

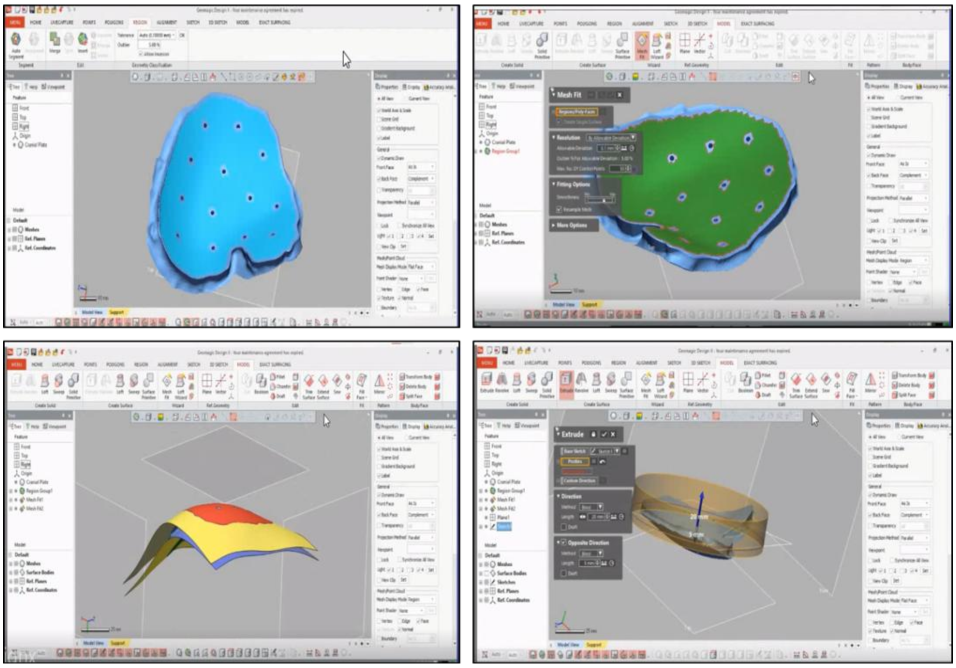

Figure 6: Conversion of STL to STEP file

Tetrahedral mesh elements discretize the cranial implant's STEP file. Every element in the file has the same 2 mm edge length. As edge length decreases, so do accuracy and file size. Figure 7 illustrates the volumetric difference between the meshed and unmeshed portions, which is shown to be within a 2% bound.

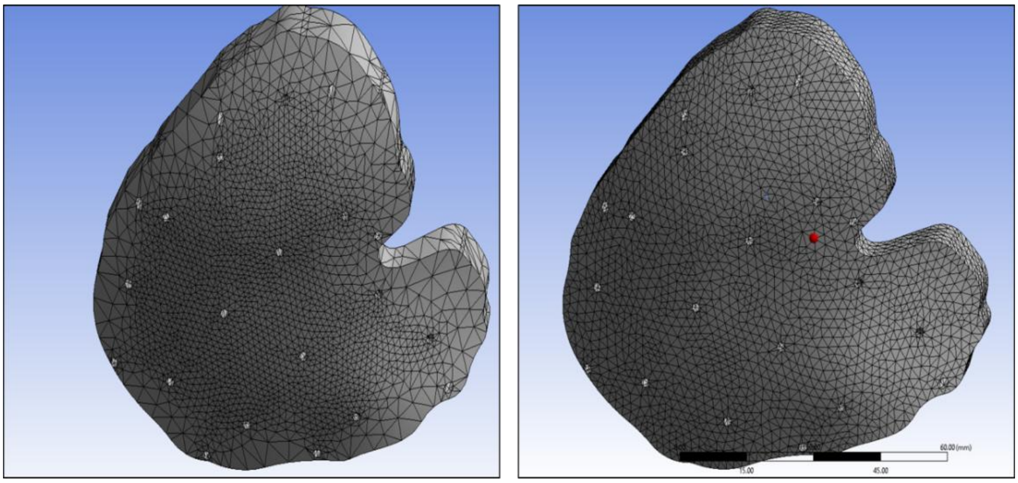

Figure 7: Part with irregular mesh and refined mesh

Comparison of mesh elements and nodes for cranial implant of two different cases is represents in Table 3.

Table 3: Comparison of meshed components for 8 fixation and 10 fixation points

	Case 1: 8 Fixation points	**Case 2: 10 Fixation point**
Element size	Edge length 2 mm	Edge length 2 mm
Number of nodes	48863	55878
Number of elements	28345	32855

III. RESULT AND DISCUSSION

To find the best implant material and fixture point design, three distinct implant materials with two different fixture point circumstances have been taken into consideration. A finite element analysis was performed on a cranial implant under static loading conditions. The edges are fastened under two different conditions—eight and ten fixation points—because the implant is intended to be anchored on the skull. The craniospinal compartment is a closed system that contains a defined volume of neural tissue, blood, and cerebrospinal fluid. The implant fixation points enable the implant to respond in accordance with the developed intracranial pressure. Few literature reviews have come to the conclusion that the nominal intracranial pressure ranges from 8 to 15 mm Hg for a healthy adult. A static pressure of 15 mm Hg is delivered to the inner surface of the implant, uniformly dispersing it over the area, taking into account the intracranial pressure state. In circumstances (8-point and 10-point fixations), the solid portion experiences complete deformation and equivalent tension (von Mises stress).

Intracranial pressure deforms the implant; Figures 7 and 8 for 8 and 10 fixation points, respectively, demonstrate the generated deformation and equivalent von Mises stresses from the simulation..

Case 1: 8 fixation points			
Material	**PEEK**	**PMMA**	**Ti6Al4V**
Equivalent Stress	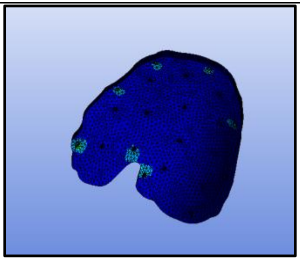	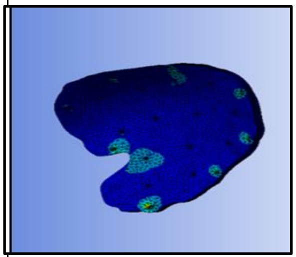	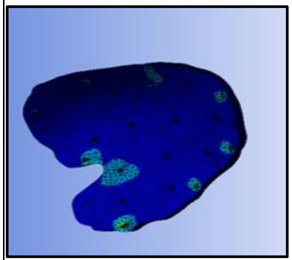
Deformation	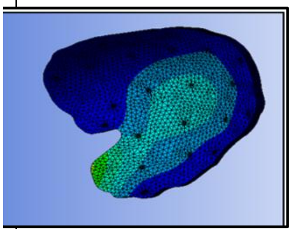	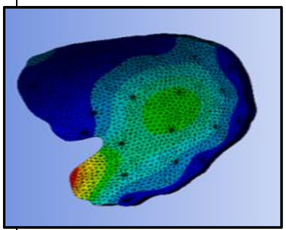	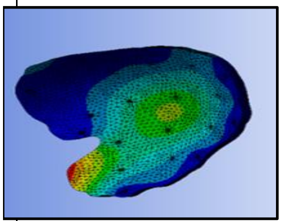

Figure 7: Equivalent stress and Maximum deformation for 8 fixation points

Case 2: 10 fixation points			
Material	**PEEK**	**PMMA**	**Ti6Al4V**
Equivalent Stress	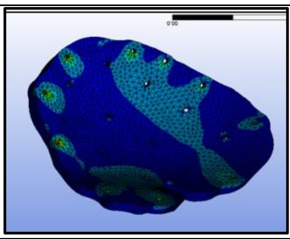	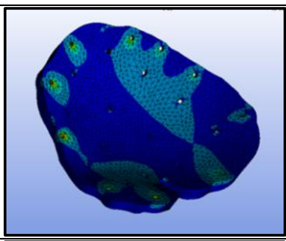	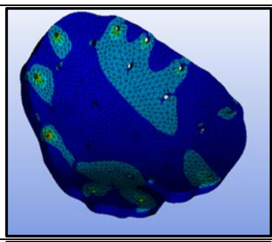
Deformation	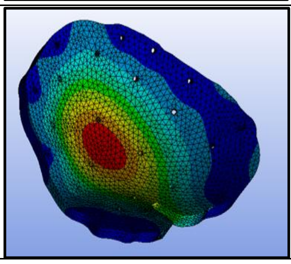	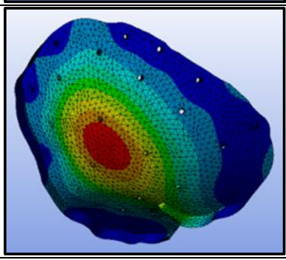	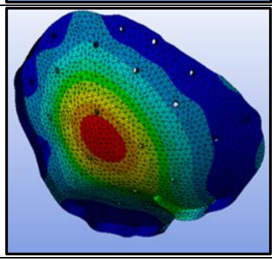

Figure 8: Equivalent stress and Maximum deformation for 10 fixation points

The simulated outcomes of a cranial implant under 15 mm Hg of intracranial pressure for 8 and 10 fixation points shown in Tables 4 and 5..

Table 4: Total Deformation and Equivalent Stress for 8 fixation Points

Case1: 8 fixation points structural analysis			
	PEEK	**PMMA**	**Ti6Al4V**
Deformation(mm)	0.0014654	0.001942	0.000051312
Equivalent Stress (MPa)	0.34965	0.36013	0.39143

Table 5: Total Deformation and Equivalent Stress for 10 fixation Points

Case2: 10 fixation points structural analysis			
	PEEK	**PMMA**	**Ti6Al4V**
Deformation(mm)	0.00070274	0.00094763	0.000026836
Equivalent Stress (MPa)	0.172731	0.17573	0.18586

Figure 9 and Figure 10 shows the comparison of maximum deformation and equivalent stress developed due to the application of intra cranial pressure on the cranial implant.

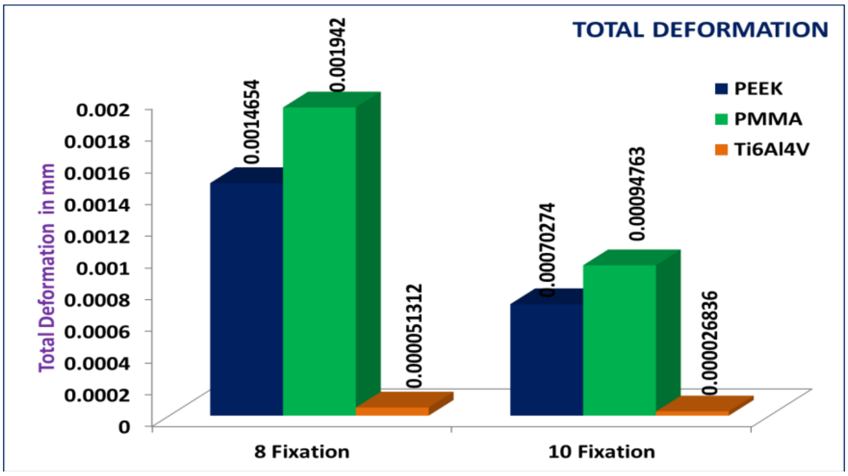

Figure 9: Comparison of deformation in 8 fixation and 10 fixation points

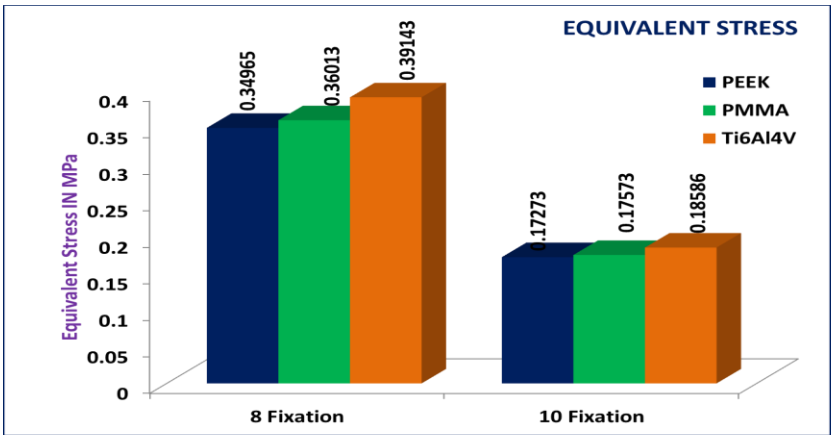

Figure 10: Comparison of equivalent stress in 8 fixation and 10 fixation points

IV. CONCLUSION

Three distinct materials—PMMA, PEEK, and titanium alloy—are taken into consideration throughout the design and development of the cranioplasty implant. The cranial implant has been sculpted from a DICOM image to an STL file, and then from a STEP file to a solid portion. On the solid cranial implant, pores were made for mineralization. An intracranial pressure of 15 mm Hg is applied to the implant's surface at fixation points 8 and 10. Finite Element Analysis has been carried out to evaluate the equivalent stress and deformation of cranial implant with boundary conditions. With both 8 and 10 fixation point condition, Ti6Al4V shows lower deformation and higher equivalent stress. When PEEK compared with PMMA, PMMA shows higher deformation (4.77% and 1.03% increase in 8 point fixation) and higher equivalent stress (1.35% and 1.03% increase in 10 point fixation) than PEEK.

V. ACKNOWLEDGEMENT

The authors are grateful to the Department of Production, Technology and Department of Rubber and Plastics Technology, MIT campus, Anna University, Chennai, India.

Funding: No funds, grants, or other support was received.

Conflicts of interest: The authors declare that they have no conflicts of interest.

REFERENCES

[1] Shah, A. M., Jung, H., & Skirboll, S. (2014). Materials used in cranioplasty: a history and analysis. Neurosurgical focus, 36(4), E19 *https://doi.org/10.3171/2014.2.FOCUS13561*

[2] Jindal, P., Chaitanya, Bharadwaja, S. S. S., Rattra, S., Pareek, D., Gupta, V., & Juneja, M. (2023). Designing cranial fixture shapes and topologies for optimizing PEEK implant thickness in cranioplasty. *Proceedings of the Institution of Mechanical Engineers, Part L: Journal of Materials: Design and Applications* 237(8):1752-1770 *https:DOI:10.1177/14644207231155761*

[3] Spetzger, U., Vougioukas, V., & Schipper, J. (2010). Materials and techniques for osseous skull reconstruction. Minimally invasive therapy & allied technologies, 19(2), 110-121. *https://doi.org/10.1016/j.msec.2016.04.101*

[4] Moncayo-Matute, F. P., Vázquez-Silva, E., Torres-Jara, P. B., Peña-Tapia, P. G., Moya-Loayza, D. P., & Abad-Farán, G. (2023, May). Mechanical analysis for personalized implant for neurocranial protection manufactured with Polymethylmethacrylate. In Journal of Physics: Conference Series (Vol. 2516, No. 1, p. 012005). IOP Publishing. *https://DOI 10.1088/1742-6596/2516/1/012005*

[5] Eufinger, H., & Saylor, B. (2001). Computer‐ assisted Prefabrication of Individual Craniofacial Implants. AORN journal, 74(5), 648-654. *https://doi.org/10.1016/S0001-2092(06)61763-8*

[6] Gautam, K. L., & Bhaskar, J. (2023). A review on 3D printed implant for oral and maxillofacial surgery. Materials Today: Proceedings. *https://doi.org/10.1016/j.matpr.2023.03.409*

[7] Salmi, M., Tuomi, J., Paloheimo, K. S., Björkstrand, R., Paloheimo, M., Salo, J., ... & Mäkitie, A. A. (2012). Patient‐ specific reconstruction with 3D modeling and DMLS additive manufacturing. Rapid Prototyping Journal, 18(3), 209-214. *https://doi.org/10.1108/13552541211218126*

[8] Msallem, B., Beiglboeck, F., Honigmann, P., Jaquiéry, C., & Thieringer, F. (2017). Craniofacial reconstruction by a cost-efficient template-based process using 3D printing. Plastic and reconstructive surgery Global open, 5(11). *https://doi: 10.1097/GOX.0000000000001582*

[9] Moiduddin, K., Mian, S. H., Ameen, W., Alkhalefah, H., & Sayeed, A. (2021). Feasibility study of the cranial implant fabricated without supports in electron beam melting. Metals, 11(3), 496. *https://doi.org/10.3390/met11030496*

[10] Gill, D. K., Walia, K., Rawat, A., Bajaj, D., Gupta, V. K., Gupta, A., ... & Jindal, P. (2018). 3D modelling and printing of craniofacial implant template. Rapid Prototyping Journal, 25(2), 397-403. *https://doi.org/10.1108/RPJ-12-2017-0257*

[11] Sharma, N., Aghlmandi, S., Dalcanale, F., Seiler, D., Zeilhofer, H. F., Honigmann, P., & Thieringer, F. M. (2021). Quantitative assessment of point-of-care 3D-printed patient-specific polyetheretherketone (PEEK) cranial implants. International Journal of Molecular Sciences, 22(16), 8521. *https://doi.org/10.3390/ijms22168521*

[12] Sharma, N., Aghlmandi, S., Cao, S., Kunz, C., Honigmann, P., & Thieringer, F. M. (2020). Quality characteristics and clinical relevance of in-house 3D-printed customized polyetheretherketone (PEEK) implants for craniofacial reconstruction. Journal of clinical medicine, 9(9), 2818. *https://doi.org/10.3390/jcm9092818*

[13] Ruiz-Huerta, L., Almanza-Arjona, Y. C., Caballero-Ruiz, A., Castro-Espinosa, H. A., Díaz-Aguirre, C. M., & Echevarria y Perez, E. (2016). CAD and AM-fabricated moulds for fast cranio-maxillofacial implants manufacture. Rapid Prototyping Journal, 22(1), 31-39. *https://doi.org/10.1108/RPJ-03-2014-0032*

[14] Lewin, S., Fleps, I., Neuhaus, D., Öhman-Mägi, C., Ferguson, S. J., Persson, C., & Helgason, B. (2020). Implicit and explicit finite element models predict the mechanical response of calcium phosphate-titanium cranial implants. journal of the mechanical behavior of biomedical materials, 112, 104085. *https://doi.org/10.1016/j.jmbbm.2020.104085*

[15] Persson, J., Helgason, B., Engqvist, H., Ferguson, S. J., & Persson, C. (2018). Stiffness and strength of cranioplastic implant systems in comparison to cranial bone. Journal of Cranio-Maxillofacial Surgery, 46(3), 418-423. *https://doi.org/10.1016/j.jcms.2017.11.025*

[16] Huang, M. T., Juan, P. K., Chen, S. Y., Wu, C. J., Wen, S. C., Cho, Y. C., ... & Ou, K. L. (2019). The potential of the three-dimensional printed titanium mesh implant for cranioplasty surgery applications: Biomechanical behaviors and surface properties. Materials Science and Engineering: C, 97, 412-419. *https://doi.org/10.1016/j.msec.2018.11.075*

[17] Phanindra Bogu, V., Ravi Kumar, Y., & Kumar Khanra, A. (2017). Homogenous scaffold-based cranial/skull implant modelling and structural analysis—unit cell algorithm-meshless approach. Medical & Biological Engineering & Computing, 55, 2053-2065. *https://doi.org/10.1007/s11517-017-1649-3*

[18] Volpe, Y., Furferi, R., Governi, L., Uccheddu, F., Carfagni, M., Mussa, F., ... & Genitori, L. (2018). Surgery of complex craniofacial defects: A single-step AM-based methodology. Computer Methods and Programs in Biomedicine, 165, 225-233. *https://doi.org/10.1016/j.cmpb.2018.09.002*

[19] Todorov, G., Nikolov, N., Sofronov, Y., Gabrovski, N., Laleva, M., & Gavrilov, T. (2019). Computer aided design of customized implants based on CT-Scan data and virtual prototypes. In Future Access Enablers for Ubiquitous and Intelligent Infrastructures: 4th EAI International Conference, FABULOUS 2019, Sofia, Bulgaria, March 28-29, 2019, Proceedings 283 (pp. 339-346). Springer International Publishing. *https://doi.org/10.1007/978-3-030-23976-3_30*

[20] Dérand III, P., Rännar, L. E., & Hirsch, J. M. (2012). Imaging, virtual planning, design, and production of patient-specific implants and clinical validation in craniomaxillofacial surgery. Craniomaxillofacial trauma & reconstruction, 5(3), 137-143. *https://doi.org/10.1055/s-0032-1313357*

[21] Gatto, M. L., Groppo, R., Bloise, N., Fassina, L., Visai, L., Galati, M., ... & Mengucci, P. (2021). Topological, mechanical and biological properties of Ti6Al4V scaffolds for bone tissue regeneration fabricated with reused powders via electron beam melting. Materials, 14(1), 224. *https://doi.org/10.3390/ma14010224*

[22] Ng, Z. Y., Ang, W. J. J., & Nawaz, I. (2014). Computer-designed polyetheretherketone implants versus titanium mesh (±acrylic cement) in alloplastic cranioplasty: a retrospective single-surgeon, single-center study. Journal of Craniofacial Surgery, 25(2), e185-e189. https://DOI: *10.1097/SCS.0000000000000623*

[23] Morales-Gómez, J. A., Garcia-Estrada, E., Leos-Bortoni, J. E., Delgado-Brito, M., Flores-Huerta, L. E., Adriana, A., ... & de León, Á. R. M. P. (2018). Cranioplasty with a low-cost customized polymethylmethacrylate implant using a desktop 3D printer. Journal of neurosurgery, 130(5), 1721-1727. https://doi.org/10.3171/2017.12.JNS172574

[24] Ridwan-Pramana, A., Marcián, P., Borák, L., Narra, N., Forouzanfar, T., & Wolff, J. (2016). Structural and mechanical implications of PMMA implant shape and interface geometry in cranioplasty–A finite element study. Journal of Cranio-Maxillofacial Surgery, 44(1), 34-44. https://doi.org/10.1016/j.jcms.2015.10.014

[25] Borie, E., Orsi, I. A., Yoshito Noritomi, P., & Takanori Kemmoku, D. (2016). Three-Dimensional Finite Element Analysis of the Biomechanical Behaviors of Implants with Different Connections, Lengths, and

Diameters Placed in the Maxillary Anterior Region. International Journal of Oral & Maxillofacial Implants, 31(1). https://doi.org/10.11607/jomi.4120

[26] Abouel Nasr, E., Al-Ahmari, A. M., Moiduddin, K., Al Kindi, M., & Kamrani, A. K. (2017). A digital design methodology for surgical planning and fabrication of customized mandible implants. Rapid Prototyping Journal, 23(1), 101-109. https://doi.org/10.1108/RPJ-11-2014-0157

[27] Oh, J. H. (2018). Recent advances in the reconstruction of cranio-maxillofacial defects using computer-aided design/computer-aided manufacturing. Maxillofacial plastic and reconstructive surgery, 40(1), 2. https://doi.org/10.1186/s40902-018-0141-9